Polish J. Chem., **78**, 973–985 (2004)

Perfluoroalkyl-*n*-eicosanes at the Air–Water Interface – A Monolayer Study

by M. Broniatowski and P. Dynarowicz-Łątka*

Jagiellonian University, Faculty of Chemistry, Ingardena 3, 30-060 Kraków, Poland

(Received April 6th, 2004; revised manuscript May 5th, 2004)

Perfluoroalkyl-*n*-eicosanes of the general formula $F(CF_2)_m(CH_2)_{20}H$, where m = 4,6, 8,10,12 were spread at the air/water as Langmuir monolayers and studied at different experimental conditions, such as spreading volume, subphase temperature and compression speed. The Langmuir monolayer experiments (π-A isotherms) have been complemented with quantitative Brewster angle microscopy results, which enabled estimation of the film thickness at different stages of compression. Although the investigated molecules do not possess any polar group and are purely hydrophobic, they form stable monomolecular layers at the free water surface. The negative sign of the measured surface potential, ΔV, evidences for the orientation of the molecules with their perfluorinated parts exposed towards the air, independently of the length of the perfluorinated moiety. The relative intensity measurements allow one to conclude that the molecules with shorter perfluorinated part (F4H20, F6H20 and F8H20) are oriented almost vertically (in respect to the interface) in the vicinity of film collapse, while F10H20 and F12H20 are tilted to the water surface.

Key words: semifluorinated alkanes, Langmuir monolayers, surface potential, Brewster angle microscopy, air/water interface

The amphiphatic molecular structure, namely a strongly polar headgroup and sufficiently long hydrophobic moiety, had been believed necessary for Langmuir monolayer formation at the air-water interface, until the work of Gaines [1], proving the film-forming properties of semifluorinated n-alkanes (abbreviated as SFA). Such compounds, of the general formula $H(CH_2)_n$-$(CF_2)_mF$ (abbreviated as HnFm), consist of a linear hydrocarbon segment linked to a fluorocarbon chain. These two constituting units are highly incompatible, which arises from a very different physical and mechanical properties of hydrogenated and perfluorinated hydrocarbons [2,3]. Namely, fluorine atoms are bigger than hydrogens, which results in a larger cross-sectional area for perfluoroalkyl chains in comparison to hydrocarbons (28.3 and 18.5 $Å^2$/molecule, respectively) [4]. To minimize steric hindrance, perfluorinated chains adopt an all-trans helical conformation, causing enhanced chain stiffness [5], contrary to polymethylene chains, which are granted conformational freedom. Additionally, fluorine atoms are more electronegative than hydrogens, and form a dense electron shield around the carbon backbone. Perfluorinated chains are

* Corresponding author: Tel. +48-12-6336377 ext. 2236; Fax: +48-12-6340515;
E-mail: ucdynaro@cyf-kr.edu.pl

also less polarizable, as compared to their hydrogenated analogues, which leads to weaker van der Waals attraction forces between neighboring molecules. Therefore, alkyl and fluorinated hydrocarbons differ significantly in the density of cohesive energy. Fluorinated compounds are more hydrophobic than their hydrogenated homologues [6]. In consequence, as compared to ordinary surfactants, the fluorinated derivatives are significantly more surface-active [7]. Regarding Langmuir monolayer formation, shorter-chain fluorinated amphiphiles are capable of a film formation at the air/water interface as compared to their hydrogenated analogues [8,9].

The presence of two opposing segments within one molecule makes semifluorinated alkanes a very interesting class of compounds, which exhibit a particular behavior in solutions and at interfaces. Their highly asymmetric structure, arising from the incompatibility of the both constituent parts, results in surface activity of these molecules (so-called *primitive surfactants*) when dissolved in organic solvents [10–15], and allows for the Langmuir monolayer formation if spread at the air/water interface [16,17], despite of the absence of the polar group.

Recently, semifluorinated alkanes have been a subject to many studies concerning their structure and physicochemical properties in bulk phase, however, only few articles [16–18] deal with their film-forming properties at interfaces.

This study provides a comparison of film forming properties of different perfluoroalkyl-*n*-eicosanes of a general formula $F(CF_2)_m(CH_2)_{20}H$, where m = 4,6,8,10 and 12. Langmuir monolayers of these selected SFA are characterized herein by surface pressure (π) and electric surface potential – area (ΔV) measurements complemented with quantitative Brewster angle microscopy.

EXPERIMENTAL

Following compounds: F4H20, F6H20, F8H20, F10H20 and F12H20 were synthesized according to the procedure described elsewhere [19]. Perfluorooctyl and perfluorobutyl iodides (98%) were purchased from Aldrich, while perfluorohexyl and perfluorodecyl iodides (99%) were supplied by Fluorochem. Perfluorododecyl iodide was supplied by Exfluor (USA). N-eicosene (90%) was purchased from Fluka. All perfluorinated iodides were used without purification, whereas n-eicosene was throughly purified before use. The purity of obtained perfluoalkyleicosanes were *ca*. 99% (^{1}H NMR, elemental analysis, mass-spectrometry). The spreading solutions for Langmuir experiments were prepared by dissolving each compound in chloroform (Aldrich, HPLC grade) with a typical concentration of *ca.* 1–1.5 mg/mL. In a typical experiment, 50–100 mL of chloroform solution was spread with a Microman Gilson microsyringe, precise to ± 0.2 μL. After spreading, the monolayers were left for 10 min for solvent evaporation, and afterwards compressed with a barrier speed of 25 cm^2/min, unless otherwise specified.

Ultrapure water (produced by a Nanopure water purification system coupled to a Milli-Q water purification system, resistivity = 18.2 MΩ · cm) was used as a subphase. The subphase temperature was controlled to within 0.1ºC by a circulating water system from Haake. Experiments were carried out with a single barrier NIMA 601 trough (Coventry, U.K.) (total area = 550 cm^2) placed on an anti-vibration table. Surface pressure was measured with the accuracy of ±0.1 mN/m using a Wilhelmy plate made from chromatography paper (Whatman Chr1) as the pressure sensor. The monolayer stability was verified by monitoring the change in surface pressure while holding the area constant. Surface potential measurements (accuracy ± 10 mV) were performed with the Kelvin probe (model KP2, NFT, Germany)

mounted on a NIMA trough. Both surface pressure-area and electric surface potential-area isotherms reported here are the averages of at least three experiments.

Relative intensity measurements were performed with Brewster angle microscope (BAM2 plus, NFT, Germany), equipped with a 30 mW laser emitting *p*-polarized light at 690 nm wavelength. The incident light was reflected off the air/water interface at approximately 53.1º (Brewster angle). At the Brewster angle:

$$I = \left| R_p \right|^2 = C\, d^2 \qquad (1)$$

where I is the relative intensity, C is a constant, d is the film thickness, and R_p is the p-component of the light [20].

RESULTS AND DISCUSSION

The surface pressure – area (π-A) isotherms of the investigated perfluoroalkyl-*n*-eicosanes are presented in Figure 1, while such parameters as: lift-off area of surface pressure (A_o), area/molecule corresponding to the film collapse and collapse pressure are gathered in Table 1. At large areas the surface pressure value oscillates around zero, and upon compression at areas between 35–30 (Å^2/molecule) starts to increase. For all the investigated SFA, the monolayer collapse occurs at *ca*. 22–23 (mN/m) (except for F12H20 which collapses at 19.7 mN/m). Collapse pressures for monolayers formed by F4H20, F6H20 and F8H20 lie between 9.5 and 12.6 mN/m, whereas films from F10H20 and F12H20 are characterized by higher collapse pressures (16.7 and 21.9 mN/m, respectively). Values of collapse pressures together with other characteristic parameters for the investigated monolayers are compiled in Table 1.

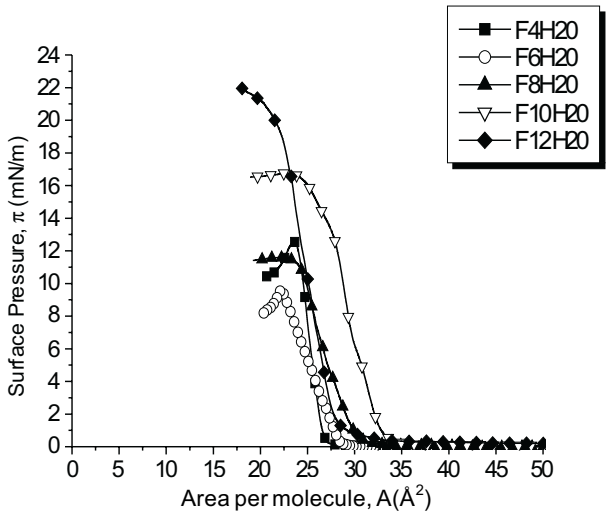

Figure 1. Surface pressure (π) – area (A) isotherms of the investigated SFA spread at the water/air interface at 20°C; compression speed: 25 cm^2/min.

Table 1. Characteristic parameters for Langmuir monolayers of the investigated SFA.

Compound	A_0 (Å^2/molec.)	A_{coll} (Å^2/molec)	π_{coll} (mN/m)	C_S^{-1} (mN/m)	A_{crit} (Å^2/molec)	$\mu_{A\ min}$ (D)	A_{min} (Å^2/molec)	I/I_0
F4H20	28.8	23.5	12.6	131.6	45.6	–0.38	32.6	36.0
F6H20	29.9	22.2	9.6	44.2	42	–0.50	32.1	33.0
F8H20	33.5	22.4	11.6	63.0	40.7	–0.56	32.6	35.2
F10H20	36.0	23.1	16.7	106.0	46.9	–0.65	36.4	18.8
F12H20	34.7	19.7	21.9	85.1	34.9	–0.57	25.4	22.4

A_0 – lift-off area of surface pressure
A_{coll} – area/molecule corresponding to the film collapse
π_{coll} – collapse pressure
C_S^{-1} – compression modulus
A_{crit} – critical area
$\mu_{A\ min}$ – minimum value of the apparent dipole moment
A_{min} – area/molecule corresponding to $\mu_{A\ min}$
$(I/I_0)_{coll}$ – value of relative intensity at the collapse

For all the studied perfluoroalkyl-*n*-eicosanes the compression modulus values (reciprocal of compressibility, defined as $C_S^{-1} = A\,d\pi/dA$) were calculated and plotted as a function of surface pressure (Figure 2). Compression modulus has been frequently used by many authors to classify the state of Langmuir monolayers into one of several possible categories [21–23]. Namely, the liquid – expanded state of a monolayer is characterized by C_S^{-1} values within the limits of 12.5–50 mN/m, liquid state: 50–100 mN/m, liquid condensed: 100–250 mN/m, and solid state: above 250 mN/m. Using this criterion, the state of monolayers from perfluoroalkyl-*n*-eicosanes can be classified as a liquid, with the exception of F4H20, which forms a liquid-condensed monolayer.

The influence of different experimental conditions on the π-A dependence was investigated in all the cases. The course of π-A isotherms was found to be independent of such experimental conditions as: speed of compression (from 10 to 100 cm^2/min), number of molecules at the water/air interface (from 1×10^{16} to 1×10^{17} molecules deposited onto water subphase) and spreading solvent (such as: chloroform, hexane, isooctane and toluene), however, a strong temperature dependence has been observed. Figure 2 displays isotherms for the investigated SFA at three different temperatures

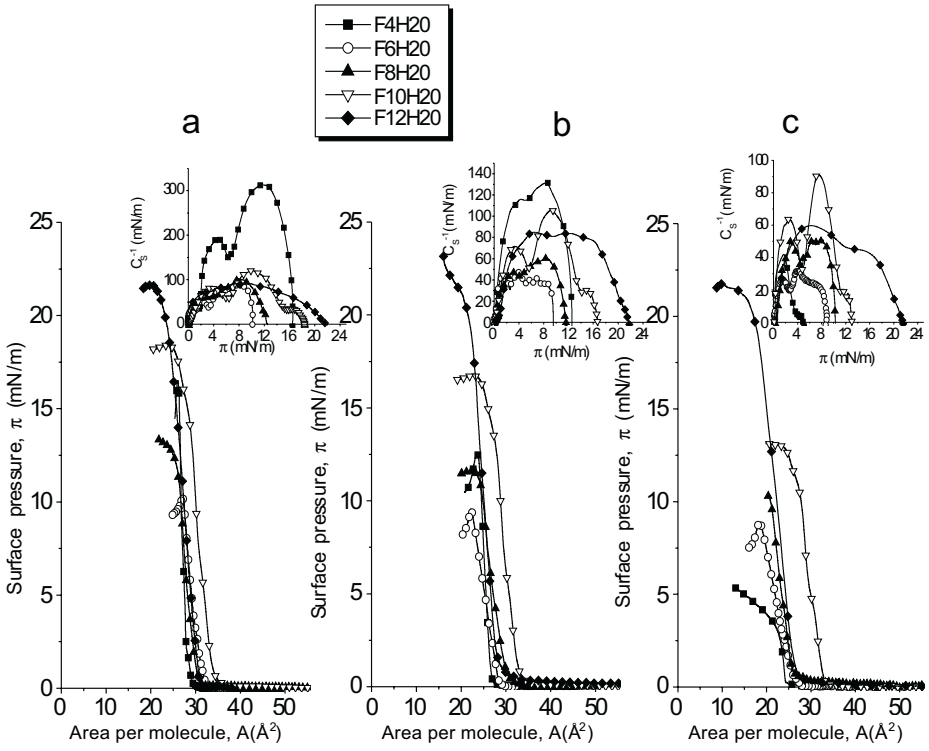

Figure 2. The influence of subphase temperature on the π-A isotherms of the investigated SFA: a) T = 10°C; b) T = 20°C; c) T = 30°C, together with the corresponding compression modulus (C_S^{-1}) – surface pressure (π) plots (inset).

(10, 20, 30°C – Fig. 3 a, b, c respectively) together with respective $C_S^{-1} = f(\pi)$ plots. The collapse pressure decreases with rising temperature, while the lift-off area and the general shape of the isotherm remains nearly the same in all three cases. Only F4H20 behaves differently, as its isotherm has a different course at 30°C as compared to lower temperatures. More pronounced differences can be observed in the $C_S^{-1} = f(\pi)$ plots for this particular compound. At 10°C, the maximum C_S^{-1} is achieved at 312 mN/m, which is a typical value for a monolayer in the solid state, while the value of 130 mN/m, measured at 20°C, corresponds to the liquid-condensed state of F4H20 film. Finally, the value of *ca*. 40 mN/m, recorded at 30°C, characterizes a liquid-expanded monolayer. For other investigated here SFA, the changes in $C_S^{-1} = f(\pi)$ plots with temperature are less pronounced, *i.e.* the monolayer state changes from a liquid to liquid expanded upon temperature increase.

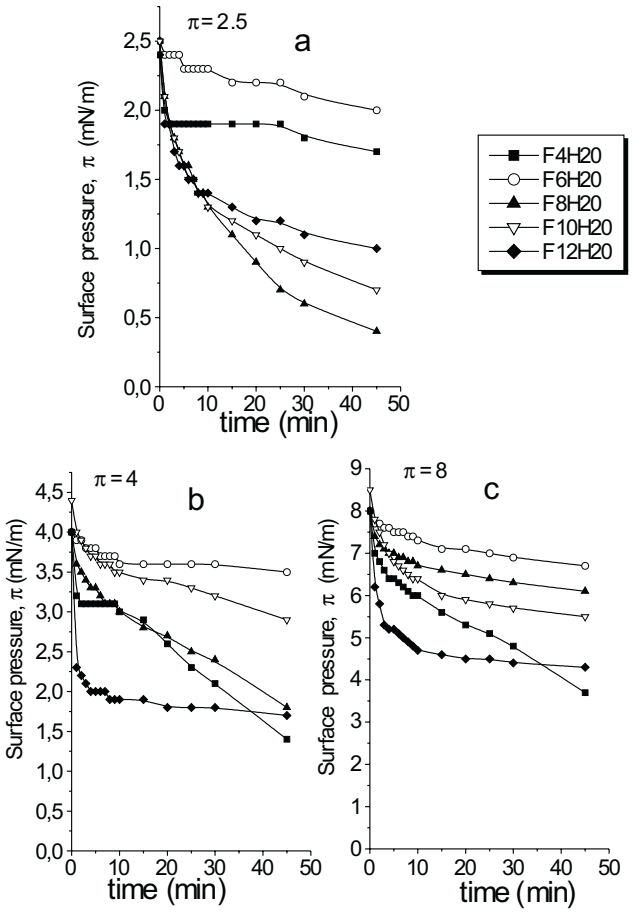

Figure 3. Stability of the monolayers of investigated SFA at different surface pressure (π) values: a) π = 2.5 mN/m; b) π = 4 mN/m; c) π = 8 mN/m.

We have also investigated thoroughly the stability of monolayers formed by perfluoroalkyl-*n*-eicosanes at the air/water interface. Films of SFA were compressed to a particular value of surface pressure (typically 2.5, 4 and 8 mN/m) and the barrier was stopped. Then, the decay of π was monitored with time (Figure 3 a,b,c respectively). Independently of surface pressure region, the monolayers formed by F6H20 are found to be most stable of all the investigated here compounds. At $\pi_0 = 2.5$ mN/m, the stability of F4H20 monolayer is high, while at higher π values it decreases significantly. In the case of F12H20, the surface pressure dropped steeply immediately after the compression had been stopped, but in 10 minutes it got stabilized at the level of *ca*. 50% of its initial value. The stabilities of the monolayers formed by F8H20 and F10H20 lie between the two extremes, namely F6H20 (upper limit) and F12H20 (lower limit).

In an independent experiment, the subsequent compression-expansion cycles (with the limiting π values mentioned above) were carried out. No hysteresis of the π-A isotherms was noticed during 5 compression-expansion cycles for all the investigated monolayers.

The electric surface potential, ΔV, was measured simultaneously with π-A isotherms, and the results are summarized in Figure 4. In general, the change of surface potential is observed at larger areas as compared to the surface pressure lift-off, *i.e*. between 35 and 50 Å^2/molecule (so-called *critical area*) [24]. Upon compression, ΔV drops, initially very steeply, achieving a point of inflection before the surface pressure starts to rise and upon further compression the drop of surface

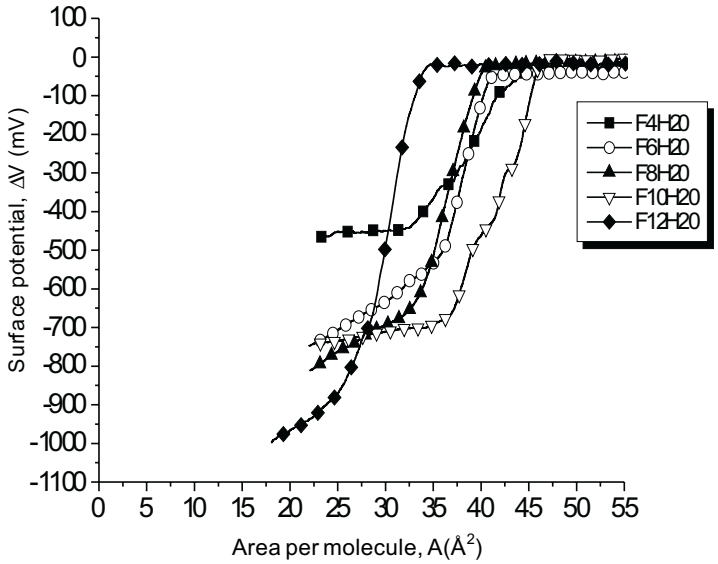

Figure 4. Electric surface potential (ΔV) – area (A) dependences for the investigated SFA.

potential is slower. A semi-quantitative analysis of the surface potential isotherm was made. Using the Helmholtz equation [21] in the form:

$$\Delta V = \mu_{\perp}/(A\varepsilon\varepsilon_0) \quad (2)$$

where $\mu_{\perp}$ is the vertical component of the dipole moment (so-called *effective* dipole moment), A is the area per molecule, while ε_0 and ε are permittivities of vacuum and monolayer, respectively, one may calculate the apparent dipole moment $\mu_A = \mu_{\perp}/\varepsilon$ at different stages of compression. The results are presented in Fig. 5. Simultaneously with the electric surface potential, the apparent dipole moment decreases and reaches its minimum at molecular areas close to the point of inflexion in the ΔV – A plot, and afterwards it increases. $\mu_{A\ min}$ values are collected in Table 1 together with the area corresponding to the minimum and critical area values.

For further quantitative analysis, the relative reflectivity (I/I_o) was measured along with the π-A isotherms for all investigated SFA and presented in Figure 6, while the I/I_0 values in the vicinity of film collapse are collected in Table 1. The relative intensities start to increase at slightly larger areas as compared to the surface pressure lift-off, and rises steeply, reaching its maximum at areas close to film collapse.

All the presented here perfluoroalkyl-*n*-eicosanes form a liquid-type floating monolayer when spread at the water-air interface. Only F4H20 forms more condensed monolayers, especially at lower subphase temperatures. This fact can be interpreted as a consequence of different molecular structure of F4H20 as compared to other perfluoroalkyl-*n*-eicosanes. The perfluorinated chain is known to have a

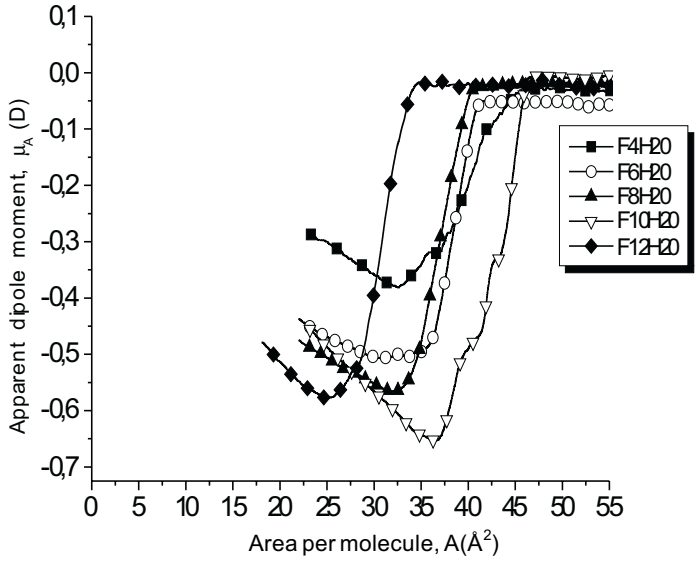

Figure 5. Apparent dipole moment (μ_A) – area (A) dependences for the investigated SFA.

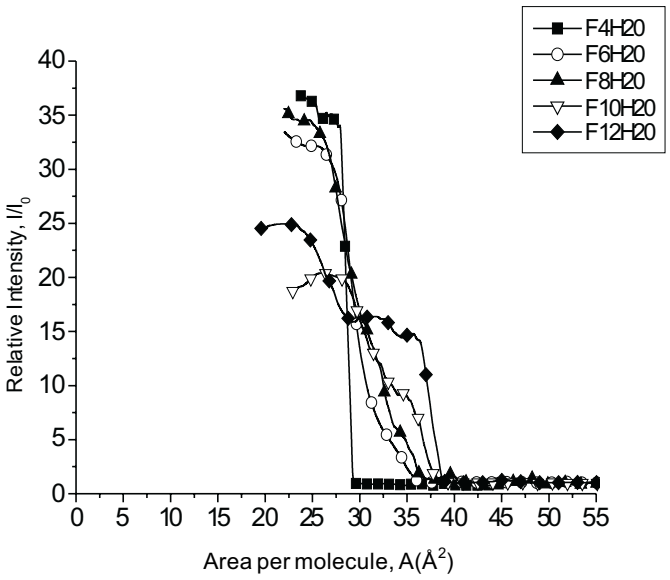

Figure 6. Relative intensity (I/I_0) – area (A) dependences for the investigated SFA.

helical structure, as illustrated in Fig. 7b, contrary to the hydrogenated moiety which adopts a flat, all-trans conformation (Fig. 7 c) [25]. However, the perfluorobutyl fragment in F4H20 is too short to form a helix, and therefore its most probable structure is a planar all-trans conformation. In consequence, F4H20 molecules can be aligned in a more closely packed arrangement in the monolayer as compared to SFA of longer perfluorinated part.

The fact that the π-A isotherms are independent of such experimental conditions as: the velocity of spreading, number of spread molecules and spreading solvents corroborates satisfactory film-forming properties of perfluoalkyl-*n*-eicosanes, which are also proved by the lack of hysteresis in subsequent compression – decompression cycles.

The temperature dependence of the π-A isotherm characteristic together with the results of monolayers stability experiments can both be explained by the fact that SFA have a significant dipole moments (*ca*. 2.8 D) and are slightly soluble in polar solvents such as methanol or even water [19,26,27]. With rising the temperature, SFA solubility may increase, which can cause the lift-off area to shift towards lower area/molecule values. A distinct behavior of F4H20 as compared to other presented here perfluoroalkyl-*n*-eicosanes consists in the fact that a change in temperature by 10°C causes profound alterations in the state of F4H20 monolayer. This can be attributed to a low melting point of F4H20 (*ca*. 35°C) in contrast to other SFA studied herein. 30° is a temperature close to the melting point of F4H20, and therefore at this temperature the monolayer is disordered.

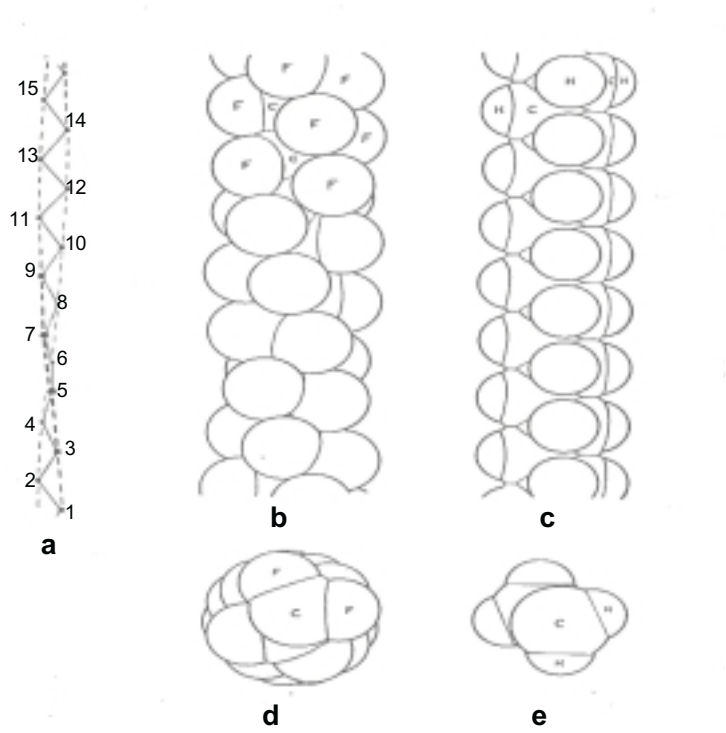

Figure 7. Crystal structure of a fluorocarbon chain compared with a hydrocarbon chain: a) twisted zigzag chain (projection of the 15/7 helix); b) 15/7 helix conformation of a fluorocarbon chain; c) all-trans (zigzag) conformation of a hydrocarbon chain, d) top side view on a fluorocarbon chain, e) top side view on a hydrocarbon chain.

Electric surface potential measurements together with the Helmholtz equation enabled us to calculate the apparent dipole moment for the investigated perfluoroalkyl-*n*-eicosanes at different stages of compression. Because SFA do not posses any polar group and are built of two hydrophobic moieties, it is not a trivial problem which of them is oriented towards the air and which is in contact with water. Gaines [1] suggests that the perfluorinated moiety is in contact with air since it is more hydrophobic than the hydrocarbon chain. However, Kim and Shin [18], on the basis of molecular dynamics analysis, proposed a mosaic structure of SFA monolayer, in which domains with oppositely directed SFA molecules are aligned in the monolayer. Such a model was supported by El Abed [17], especially in the region of large areas per molecule. In our opinion, the mosaic model is less probable than that suggested by Gaines, because negative values of the measured surface potentials indicate that the perfluorinated parts of perfluoroalkyl-*n*-eicosanes are directed towards the air. If the hydrogenated parts were exposed to the air, the measured surface potential would be positive, whereas in the case of the mosaic model, it should be around zero because of the cancellation of oppositely directed dipole vector moments.

It is a very interesting feature that, contrary to model film-forming molecules, like *i.e*. long-chain, saturated, linear fatty acids (in the case of which the maximum value of μ_A is reached in the condensed region where molecules are believed to orient vertically in respect to the surface [28]) for SFA maximum absolute value $|\mu_A|$ appears before the π-A isotherm starts to rise. According to Davies and Rideal [29] for -CF_3 ω-terminated amphiphile molecules (like ω-CF_3 carboxylic acids) the dipole moment vector is inclined to the main axis [defined as a line intersecting all the C–C bonds (all-trans configuration) in the middle of their length] at the angle of 35.25°. Therefore, when such a molecule is oriented perpendicularly to the water/air interface in a condensed monolayer the angle between the dipole moment direction and the water/air interface is 54.75° which makes the half of the tetrahedral angle. We have verified the orientation of dipole moment vector of perfluoroalkyl-*n*-eicosanes using quantum chemistry computer program (*Hyper Chem* [30]). We have performed semiempirical dipole moment computations in vacuum using PM3 approximation and eigenvector following algorithm in iteration cycles for all investigated perfluoroalkyl-*n*-eicosanes. The value of the calculated dipole moment was almost identical for all compounds (*ca*. 2.8± 0.1 D). The calculated angle between the long axis of SFA molecule and the dipole moment vector direction was 35.25°, which is in a good agreement with the value predicted previously by Davies and Rideal [29] for ω-halogen substituted amphiphiles. Large values of critical areas can be interpreted following the paper of Leite *et al.* [24]. At large areas, film molecules are well separated in a gas-liquid monolayer. In this region, both surface pressure and electric surface potential depict the value for pure water. Thus it may be assumed that the molecules lie horizontally at the surface, and a network of weak H-bonds between F atoms and water molecules can be formed. Upon compression, the hydrogen bonds break, and a rapid decrease in electric surface potential value is observed.

The plot of relative intensities I/I_0 *versus* area for all reported here SFA is presented in Fig. 6. The thickness of monolayer d is related to the relative intensity by the formula: $I = Cd^2$, where C is a constant. Consequently $I/I_0 = d^2/d_0^2$, where d_0 is the thickness of the monolayer at the beginning of compression, where one can suppose that the film forming molecules lie horizontally on the water surface. The cross-section of a SFA is 28.6 $Å^2$ [25], and thus the thickness of the horizontally oriented SFA molecule is *ca*. 6 Å (twice the radius of the rigid rod, which is often used as a model of a SFA molecule). The experimental thicknesses of a SFA monolayer at any point of the compression can be obtained by multiplication of the square root of I/I_0 by 6.

According to Viney *et al.* [31], the theoretical length of SFA molecule in all-trans configuration can be calculated from the following equation:

$$d_{theor.} = (m-1)\times 1.3 + (n-1)\times 1.25 + 1.28 + 1.1 + 0.9 \quad (3)$$

where: *m* – the number of carbon atoms in the fluorinated moiety, *n* – the number of carbon atoms in the hydrogenated moiety, 1.28 – the CH_2-CF_2 bond contribution (average of 1.25 and 1.3), 1.1 – the terminal C–F bond contribution and 0.9 – the terminal C–H bond contribution.

In the above equation Viney and co-authors assume that: C–C bond in the hydrogenated part is 1.53 Å long, while C–C distance in the fluorocarbon part is 1.60 Å, and all valence angles in the hydrogenated part are assumed to be tetrahedral. In the calculations [31] the authors approximate the 15/7 helix structure of the perfluorinated fragment to the planar all-trans conformation. It seems to be an acceptable assumption (see Figure 7a) and was successfully applied by Lo Nostro *et al*. [32] in their paper.

Both theoretical lengths (d_{theor}) and experimental thicknesses (d) of investigated perfluoroalkyl-*n*-eicosanes moieties and their monolayers, respectively, have been calculated and presented in Table 2.

Table 2. Comparation of the theoretical length of SFA molecules with experimentally estimated thickness of their monolayers.

Compound	d_{theor} (Å)	d (Å)
F4H20	30.9	36.0
F6H20	33.5	34.5
F8H20	36.1	35.6
F10H20	38.7	26.0
F12H20	41.3	28.4

d_{theor} – theoretical length of a SFA molecule
d – experimentally estimated thickness of the monolayer

For F6H20 and F8H20 molecules the experimentally evaluated thickness of their monolayers at the air/water interface are in very good agreement with the theoretical molecular length calculated according to Viney [31]. For F4H20 the evaluated thickness is *ca*. 8% larger than the theoretical length of this molecule, but this discrepancy can be ascribed to the experimental error. All the three molecules seem to be oriented perpendicularly to the water surface in the vicinity of the film collapse.

The situation for F10H20 and F12H20 is different because experimentally estimated monolayer thickness is *ca*. 32% thinner than the theoretical length of the molecule. Similar tendencies were observed by us for other perfluorodecyl and perfluorododecyl-*n*-alkanes. To explain this phenomenon it can be suggested that molecular tilt is responsible for the difference between d_{theor} and d. Consequently, the tilt angle φ (defined as an angle between the main axis of the film forming molecule and the subphase normal) is *ca*. 60° for F10H20 and F12H20.

Acknowledgment

The authors wish to express their gratitude to Prof. R. Soulen (Exfluor, USA) for providing perfluorododecyl iodide sample.

REFERENCES

1. Gaines G.L. Jr., *Langmuir*, **7**, 3054 (1991).
2. Jarvis N.L. and Zisman W.A, in *Encyclopedia of Chemical Technology.* Vol. 7. Wiley, NY 1966.
3. Hoffmann H. and Würz J., *J. Mol. Liq.*, **72**, 191 (1997).
4. Lo Nostro P., Ku C.Y., Chen S.H. and Lin J.S., *J. Phys.Chem.*, **99**, 10858 (1995).
5. Ha K.R., Kim J.M. and Rabolt J.F., *Thin Solid Films*, **347**, 272 (1999).
6. Tadros T.F., *J. Colloid Interface Sci*, **75**, 196 (1980).
7. Kunieda H. and Shinoda K., *J. Phys. Chem*., **80**, 2468 (1976).
8. Lehmler H.J., Jay M. and Bummer P., *Langmuir*, **16**, 10161 (2000).
9. Riess J.G., *Tetrahedron*, **58**, 4113 (2002).
10. Turberg M.P. and Brady J.E., *J. Am. Chem.Soc*., **110**, 7797 (1988).
11. Binks B.P., Fletcher P.D.I., Sager W.F.C. and Thompson R.L., *J. Mol. Liq*., **72**, 177 (1997).
12. Binks B.P., Fletcher P.D.I., Sager W.F.C. and Thompson R.L., *Langmuir*, **11**, 977 (1995).
13. Hayami Y. and Findenegg G.H., *Langmuir*, **13**, 4865 (1997).
14. Binks B.P., Fletcher P.D.I., Kotsev S.N. and Thompson R.L., *Langmuir*, **13**, 6669 (1997).
15. Marczuk P., Lang P. and Möller M., *Coll. Surf. A*, **163**, 103 (2000).
16. Huang Z., Acero A.A., Lei N., Rice S.A., Zhang Z. and Schlossman M.L., *J. Chem. Soc., Faraday Trans*., **92**, 545 (1996).
17. El Abed A., Fauré M.C., Pouzet E. and Abillon O., *Phys. Rev. E*, **65**, art. no. 051603 (2002).
18. Kim N. and Shin S., *J. Chem. Phys*., **110**, 10239 (1999).
19. Rabolt J.F., Russell T.P. and Twieg R.J., *Macromol*., **17**, 2786 (1984).
20. Azzam R.M.A. and Bashara N.M., in *Ellipsometry and Polarized Light*, 1st ed., North Holland, Amsterdam 1992.
21. Davies J.T. and Rideal E.K., in *Interfacial Phenomena*. 2nd ed, Academic Press, NY, 1963, pp. 265 and 65.
22. Harkins W.D., in *The Physical Chemistry of Surface Films*. Reinhold Publ. Corp., NY, 1952, p. 107.
23. Reis T., in *Introduction a la Chimie-Physique des Surfaces.* Dunod. París, 1952, p. 111.
24. Leite V.B.P., Cavalli A. and Oliveira O.N. Jr., *Phys. Rev. E*, **57**, 6835 (1998).
25. Bunn C.W. and Howells E.R., *Nature*, **174**, 549 (1954).
26. Napoli M., Conte L. and Gambaretto G.P., *J. Fluor. Chem*., **85**, 163 (1997).
27. Napoli M., Conte L. and Guerrato A., *J. Fluor. Chem.*, **110**, 47 (2001).
28. Vogel V. and Möbius D., *J. Colloid Interface Sci*., **126**, 408 (1988).
29. Davies J.T. and Rideal E.K., *Can. J. Chem.*, **33**, 947 (1955).
30. HyperChem Professional Release5.1, A Molecular Visualization and Simulation Software Package Hypertube Inc., Gainesville, Florida, USA, 1988.
31. Viney C., Russel T.P., Depero L.E. and Twieg R.J., *Mol. Cryst. Liq. Cryst.*, **168**, 63 (1989).
32. Lo Nostro P. and Chen S.H., *J. Phys. Chem.*, **97**, 6535 (1993).